Electrically controlled light scattering from thermoreversible liquid-crystal gels

Electrically controlled light scattering from thermoreversible liquid-crystal gels

Rob H. C. Janssen[a)]
Department of Chemical Engineering, Eindhoven University of Technology, P.O. Box 513, 5600 MB Eindhoven, The Netherlands and Department of Materials, ETH-Zentrum UNO C15, CH-8092 Zürich, Switzerland

Volker Stümpflen
Department of Chemical Engineering, Eindhoven University of Technology, P.O. Box 513, 5600 MB Eindhoven, The Netherlands

Dirk J. Broer
Department of Chemical Engineering, Eindhoven University of Technology, P.O. Box 513, 5600 MB Eindhoven, The Netherlands and Philips Research Laboratories, Prof. Holstlaan 4, 5656 AA Eindhoven, The Netherlands

Cees W. M. Bastiaansen
Department of Chemical Engineering, Eindhoven University of Technology, P.O. Box 513, 5600 NB Eindhoven, The Netherlands

Theo A. Tervoort and Paul Smith
Department of Materials, ETH-Zentrum UNO C15, CH-8092 Zürich, Switzerland

(Received 5 January 2000; accepted for publication 29 March 2000)

Thermoreversible gels of the liquid-crystal LC-E7 with 1,3:2,4-Di-O-benzylidene-D-sorbitol (DBS) form white light-scattering films that are reversibly switchable to a clear state by ac electric fields. The light scattering by the gelled films is an intrinsic material property that originates in the phase diagram of the system displaying a monotectic-type equilibrium (''mesotectic'') among a liquid, a solid, and a mesophase at extremely low concentrations of DBS. Electro-optical characteristics and demonstrated viscoelastic behavior of the films produced indicate the applicability of DBS/LC-E7 in large area scattering-based flat panel displays and projection systems. © *2000 American Institute of Physics.* [S0021-8979(00)03613-6]

I. INTRODUCTION

Of the many low molecular weight organic gelators that have been discovered over the years,[1] 1,3:2,4-di-O-benzylidene-D-sorbitol (DBS) is among the oldest and most versatile.[2,3] It is known to cause gelation in the semidilute concentration range ($\leqslant 5\%$) in a great variety of liquids ranging from chloroform[4] to ethylene glycol[5] and siloxanes.[6] Gel formation in these solvents is attributed to an association of DBS molecules into well-ordered helical aggregates[2] that interwind to form a submicron scale three-dimensional network, turning the solutions into viscoelastic solids. The helical twist of the aggregates stems from the optical purity of DBS molecules and is essential for gelation to occur;[7] in racemic mixtures of D- and L-sorbitol-based DBS molecules, crystals precipitate.[8] The effectiveness of DBS is illustrated by its commercial exploitation as a nucleating agent for polymer crystallization[9] to improve the optical clarity and mechanical properties of isotactic polypropylene.[10] Clearly, since the gelation relies on physical association processes; it can be reversed by heating the gels above their gelation temperature. Therefore, from a thermodynamics point of view, gelation by the action of DBS may be looked upon as submicron scale phase separation resulting in a well-organized $\{C_2\}$ phase (the ''crystalline'' network; 2≡DBS) that is finely dispersed in an isotropic liquid $\{L\}$ [or a birefringent phase $\{N\}$ in the case of a nematic liquid crystal (LC)].

In the current contribution we report on the ability of DBS to form electroresponsive gels with the liquid-crystal LC-E7 and show the main characteristics of a scattering-based electro-optical cell (Fig. 6). Further, a (quasibinary) phase diagram of DBS/LC-E7, based on differential scanning calorimetry (DSC) thermograms, is presented and wide angle x-ray scattering (WAXS) recordings of the structures in the different coexistence regions are shown. From the phase diagram it is concluded that the DBS/LC-E7 system displays a monotectic-type[11] three-phase equilibrium $\{L\} = \{N + C_2\}$, in which isotropic liquid coexits with a birefringent liquid $\{N\}$ and a solid-like $\{C_2\}$ phase. Previously, in Ref. 12, the term ''mesotectic'' was introduced for this type of equilibrium to denote that it is an intermediate of true monotectic, for which $\{L_1\} = \{L_2 + C_2\}$, and a eutectic $\{L_1\} = \{C_1 + C_2\}$. Of specific importance to the current work is the location of the ''mesotectic'' in the phase diagram of DBS/LC-E7, resulting in the formation of white light scattering films at all practically relevant materials compositions. This is in great contrast to other thermoreversible LC gels that have only been used in twisted nematic configurations.[12–15] Combined with demonstrated viscoelas-

[a)]Author to whom correspondence should be addressed at the Eindhoven University of Technology; electronic mail: rob@pluto.chem.tue.nl

tic behavior of gelled films and switching from and to a clear state upon application of an ac-electric field, this suggests the use of DBS/LC-E7 in large area scattering-based display applications. In this respect, the system may be regarded as an alternative to polymer dispersed liquid crystals (PDLCs),[16,17] anisotropic gels based on LC-diacrylate networks,[18] and LC phases stabilized with fumed silica particle networks.[19]

II. EXPERIMENT

A. Materials and sample and electro-optical cell preparation

DBS ($T_m = 225$ °C, $\rho = 1.04$ g/cm^3, purity>96%), with the trade name Millad 3905, was used as received from Milliken Chemical. LC-E7, a multicomponent cyanobiphenyl and terphenyl mixture (see Ref. 20 for its composition; $T_{N/I} = 60$ °C, $\rho = 1.06$ g/cm^3, $\epsilon_{\parallel} = 19$ and $\epsilon_{\perp} = 5.2$, and $\Delta n = 0.225$) was used as obtained from Merck.

Samples were prepared by dissolving milligram amounts of DBS in droplets of LC material at elevated temperatures (up to 190 °C for the samples containing the highest amounts of DBS). To check on evaporation of the components of LC-E7, sample compositions were determined by reweighting after cooling to room temperature. Gels produced were found to be stable; no weakening was observed after periods of several months.

Electro-optical cells were prepared by mounting two glass plates coated with transparent indium–tin–oxide (ITO) electrodes (type 327 735 PO from Merck) on top of each other with an UV curable sealant (UVS 91 by Norland Products, Inc.) applied to the edges, and subsequent curing. No orientation layers were used. Monodisperse silica spheres, applied to one of the plates by spin coating from a volatile alcohol dispersion (10 s at 1000 rpm), assured an 18 μm spacing between the plates. Finally, cells were rapidly filled by capillary action at temperatures well above the sol–gel transition of the particular sample.

B. Calorimetric, x-ray, mechanical, and electro-optical analysis

Calorimetric analysis was performed using a Perkin–Elmer DSC 7 DSC. Experiments were run at 10 °C/min in O-ring sealed pans (Perkin–Elmer, type No. 0319-0218), suppressing vaporization heat effects. Before sealing the filled capsules, their contents were homogenized at elevated temperatures and the composition was determined by reweighting.

Wide angle x-ray diffractograms were recorded at the European Synchrotron Radiation Facility (ESRF, Grenoble, France) on the ID11 instrument at a wavelength $\lambda = 0.72$ Å ($E = 17.3$ keV). Glass capillaries ($\phi = 2.0$ mm; by W. Müller, Germany) were filled by capillary action and placed in a sample holder equipped with a Linkam TMS92 hot stage. Temperature scans were performed at 10 °C/min. In the present work, only bare WAXS recordings are shown; no data processing was performed.

Strain-controlled dynamical mechanical analysis was performed in a Rheometrics ARES rotational viscosimeter using a plate–plate geometry ($\phi_{\text{plate}} = 25$ mm). Films of about 1 mm thick were prepared *in situ* by heating 0.5 g of material above its sol–gel temperature and subsequent cooling, while maintaining a weak positive normal force (± 0.25 N/cm^2). Each sample was examined several times at 30 °C; before each measurement, samples were reheated to erase their thermomechanical history.

Measurements were performed by recording the torque τ on the fixed upper plate of the viscosimeter, while rotating the bottom plate over angles $\alpha = \alpha_0 \sin \omega t$ at a frequency $\omega = 1.0$ rad/s low enough to guarantee that at the lowest α_0s tested, the material is well within the linear strain regime. A subsequent fit of $\{\tau, \alpha\}$ to the linear viscoelastic material equation[21,22]

$$\tau(t) = G_d \frac{\pi r^4}{2d} \alpha_0 \cos(\omega t + \delta) \tag{1}$$

allows the determination of the storage and loss moduli from $G' = G_d \cos \delta$ and $G'' = G_d \sin \delta$. In Eq. (1), the dynamic modulus $G_d(\omega, T)$ and phase shift $\delta(\omega, T)$ are frequency and temperature dependent viscoelastic parameters and the plate–plate distance d and plate radius r are known geometrical factors. During the experiment, it was carefully checked that no slip occurred at the interface of the plate and the gelled film.

Electro-optical characterization of the cells was performed with the aid of a display measurement system, DMS 703, from Autronic Melchers GmbH. 100 Hz square wave voltages were applied and varied every 0.1 s in the range 0–150 V (equipment limit) in steps of 0.5 V. Cells, placed 10 cm above a diffuser plate, were illuminated with a 100 W halogen light source and transmitted light was collected with a built-in 0.2 mm spot-size detector.

III. RESULTS AND DISCUSSION

A. Phase behavior

A (partial) phase diagram of the DBS/LC-E7 system is shown in Fig. 1(a), where the transition temperatures, as observed by DSC, are plotted *versus* the material composition (w is the weight fraction DBS). It should be noted that LC-E7 is a multicomponent mixture, and thus, an interpretation in terms of a binary phase diagram such as Fig. 1(a) is not strictly correct. Nevertheless, we believe that the phase diagram provides essential insights justifying its use. As shown, we have only examined the composition range $w \leqslant 0.35$ ($\equiv T \leqslant 200$ °C), because dissolving increased amounts of DBS requires heating to higher temperatures for which thermogravimetric analysis of the LC material shows significant weight loss.

In Fig. 1(a), which is based on the DSC melting traces shown in Fig. 2 and WAXS data shown in Fig. 3, three characteristic regions, $\{L_1\}$, $\{L_1 + C_2\}$, and $\{N + C_2\}$, separated by two characteristic transitions (□) and (● and ○) are observed. In the region $\{L_1\}$, the DBS/LC-E7 system appears as an isotropic liquid. In the other regions two phases coexist: an isotropic LC-rich liquid and a finely dispersed well-ordered network phase in the $\{L_1 + C_2\}$ region (this is the isotropic gel region);[12–15] and a birefringent LC-rich liquid and the network in the $\{N + C_2\}$ region (this is the aniso-

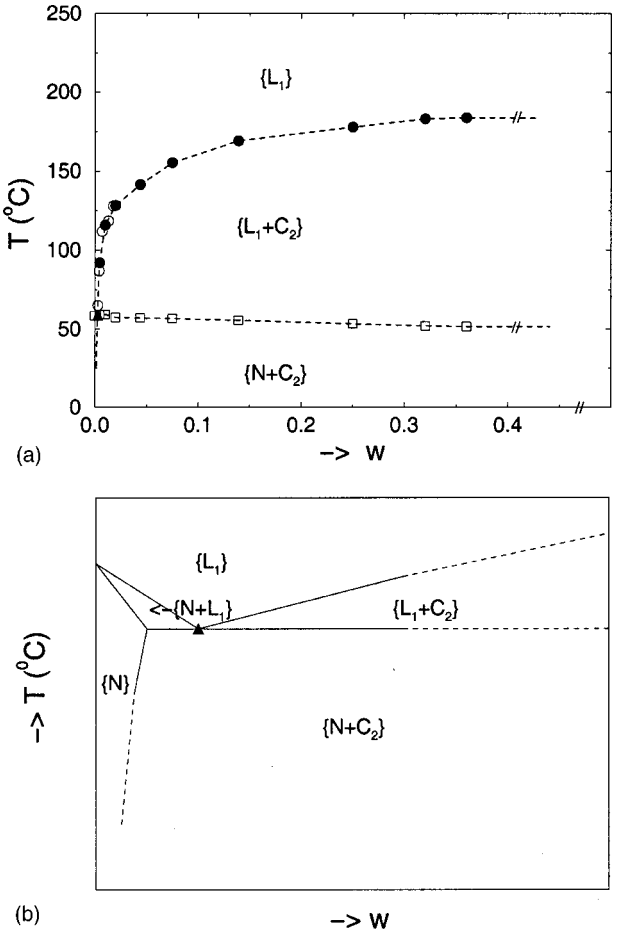

FIG. 1. (a) Phase diagram of the DBS/LC-E7 system. Transition temperatures (□), (●), were measured by DSC [see Figs. 2(a)–2(b)] and (○) by microscopic observations of ''gel melting.'' The symbol (▲) indicates the mesotectic 3-phase equilibrium $\{L_1\}=\{N+C_2\}$. (b) Schematic diagram of the DBS/LC-E7 phase behavior. The mesotectic point is indicated by (▲). Full lines represent observed transitions as condensed in (a), and dotted lines are extrapolations.

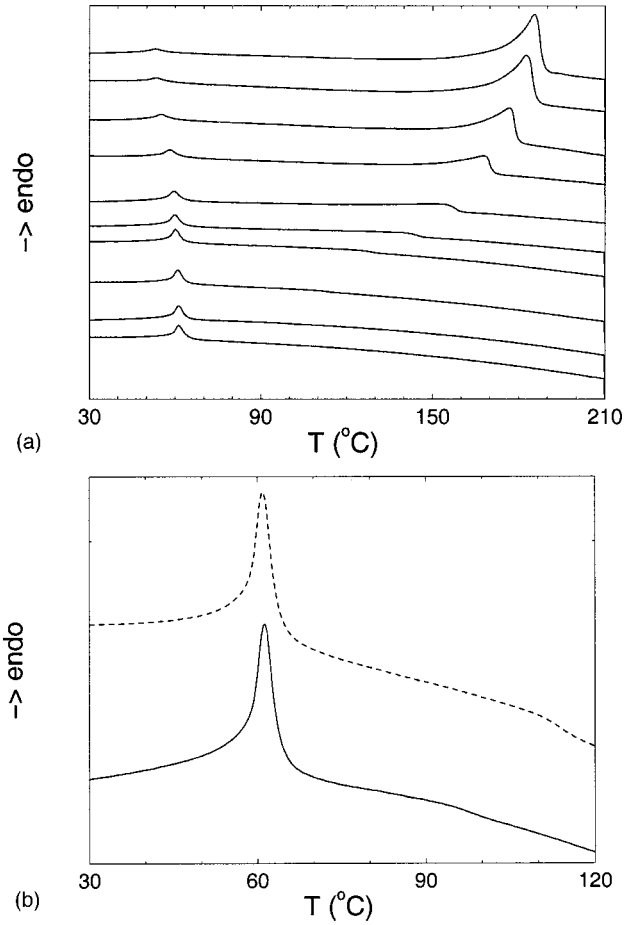

FIG. 2. (a) DSC thermograms of, from top to bottom, 36.3 wt % DBS/LC-E7; 32%; 25%; 13.9%; 7.5%; 4.5%; 2%; 1%; 0.5%; and 0% (neat E7). (b) DSC traces of 1 wt % DBS/LC-E7 (dotted line) and 0.5 wt % (solid line). Thermograms are enlarged versions of traces shown in (a) to more clearly depict the weak signals associated with the sol–gel transition at $T\approx115$ °C (1%; dotted line) and $T\approx95$ °C (0.5%; solid line).

tropic gel region).[12–15] The transitions in Fig. 1(a) correspond to, respectively, the nematic–isotropic transition of the LC-rich phase $T_{N/I}$ (□) and the sol–gel transition at which the DBS network is formed or broken T_{SG} (● and ○). The phase behavior of the DBS/E7 system has also been studied by optical microscopy which, in fact, allowed detection of gelation in samples with weight fractions DBS as low as 0.3% (DSC gave only signals down to 0.5%; see Fig. 2.

As shown in Fig. 1(a), the phase separation in the $\{N+C_2\}$ region is nearly complete, i.e., a well-ordered submicron scale $\{C_2\}$ phase coexists with a $\{N\}$ phase, consisting of nearly pure LC material. In the $\{N\}$ phase, the environment of the LC molecules is liquid-like, allowing the LC molecules to maintain their (speed of) response to an electric field. Macroscopically, on the other hand, due to the $\{C_2\}$ network, the DBS/LC-E7 system behaves as a viscoelastic solid.

In Fig. 1(a) we have also marked the location of a mesotectic three-phase equilibrium point $\{L_1\}=\{N+C_2\}$ (▲)[12] at $w\approx0.002$ and $T=60$ °C. The presence of this point in the phase diagram of DBS/LC-E7 may not be immediately obvious from the data displayed, but is a direct consequence of the indisputable existence of a $\{N+L_1\}$ coexistence region at low w, as is understood from the schematic picture in Fig. 1(b). Therefore, we are essentially dealing with the same type of phase diagram as in previously studied thermoreversible LC gels such as 12-hydroxyoctadecanoic acid (HOA)/LC-TL213[12] and other systems.[13–15]

Since the mesotectic point in the DBS/LC-E7 phase diagram is located very close to the $w=0$ axis, cooling of practically relevant material compositions, $0.0025\leqslant w\leqslant0.05$, implies passing the mesotectic point from the right hand side for which T_{SG} (●)$>T_{N/I}$ (□) (see Fig. 1). Therefore, the N/I transition occurs in a highly viscous (gelled) material, and the LC molecules cannot be oriented by weak external forces such as polyimide orientation layers to form monolithic structures, e.g., twisted nematic layers. Alternatively, the network causes micron-scale spatial director variations leading to a strongly enhanced light scattering when compared to neat LC-E7, and the light scattering thus is an intrinsic property of the material.

In principle, refractive index differences between the network and (birefringent) liquid phase may also contribute to the scattering. However, since the material becomes per-

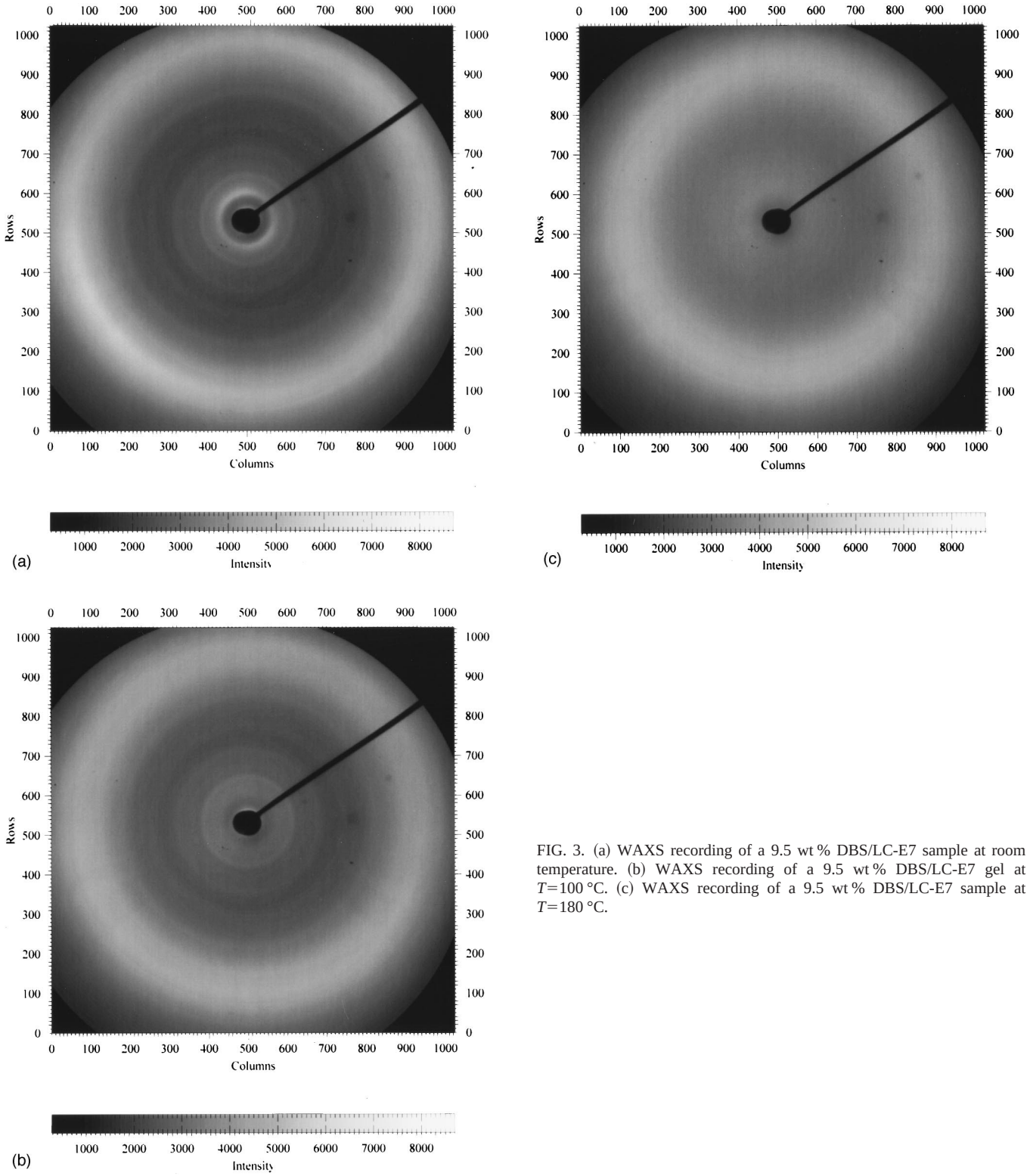

FIG. 3. (a) WAXS recording of a 9.5 wt % DBS/LC-E7 sample at room temperature. (b) WAXS recording of a 9.5 wt % DBS/LC-E7 gel at $T=100$ °C. (c) WAXS recording of a 9.5 wt % DBS/LC-E7 sample at $T=180$ °C.

fectly transparent when heated into the isotropic gel state, we believe this to be a minor effect, as also follows from the typical size of the aggregates in DBS gels ($\ll$100 nm).[2,5]

Clearly, this light scattering by DBS/LC-E7 may be exploited in smart windows or scattering based display applications such as flat panel displays, electronic paper, or projection systems. In contrast, the phase diagrams of other LC gels reveal their applicability in twisted nematic display applications: in the phase diagram of the previously studied HOA/LC-TL213 system, a mesotectic equilibrium occurs at $w\approx0.33$ and $T=70$ °C. Therefore, cooling of practically relevant compositions results in passing the mesotectic point from the left, for which $T_{N/I}>T_{SG}$ [see Fig. 1(b)]. In this case the LC molecules may be oriented, e.g., into twisted nematic configurations and subsequently gelled at a lower temperature T_{SG}.[12]

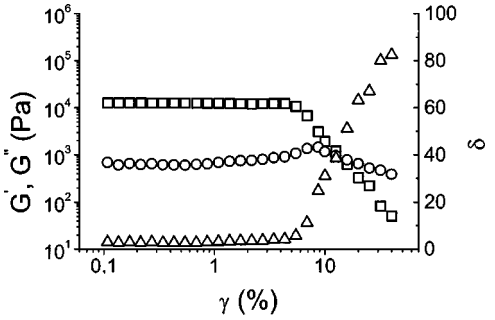

FIG. 4. Loss angle δ (△), and storage G' (□) and loss G''(○) moduli vs material strain γ of a 0.5 wt % DBS/E7 gel at $T=30$ °C. From the sudden decrease in the value of G', the maximum strain at network failure, γ_{max}, is estimated to be 0.06.

When looking at the DSC thermograms in Fig. 2, it is seen that $T_{N/I}$ decreases over 6 °C upon increasing the DBS concentration, and the decrease is accompanied by a broadening and weakening of the DSC signals. This is indicative of a weakening of order in the LC phase due to ''pore'' confinement[23] and of an increase of the fraction of LC molecules ''bound'' to the DBS strands.[24]

Finally, Fig. 3 shows WAXS recordings of structures of coexisting phases in a 9.5 wt % DBS gel at, respectively, room temperature [Fig. 3(a)], $T=100$ °C [Fig. 3(b)], and $T=180$ °C [Fig. 3(c)]. Figure 3(a), taken at room temperature, shows a recording of the anisotropic gel region in which the $\{N+C_2\}$ phases coexist. Visible are two bright, diffuse rings, originating from the $\{N\}$ phase, caused by electron density variations perpendicular to the nematic director (outer ring; corresponding to an average periodicity of $s\approx4.3$ Å) and along the director (inner ring; $s\approx25$ Å). Other rings originate from the $\{C_2\}$ phase formed by DBS. These rings tend to be sharper, indicating that DBS molecules arrange into well-ordered structures displaying relatively large correlation lengths $\xi=\lambda/\Delta\Theta$ (with Θ the scattering angle).[24] Figure 3(b) shows the structures of coexisting $\{L_1+C_2\}$ phases at $T=100$ °C in the isotropic gel region. Since the molecules constituting LC-E7 are now in the isotropic $\{L_1\}$ phase, the inner diffuse ring visible in Fig. 3(a) has vanished. The outer ring, which originates from electron density variations caused by a parallel local arrangement of neighboring LC molecules,[25] is still present. Note that the reflections of the ordered $\{C_2\}$ phase have remained unchanged when compared to Fig. 3(a). Upon further heating to $T=180$ °C these also disappear [Fig. 3(c)], indicating that the gel has ''melted.'' Therefore, although the Bragg-type reflections visible in Figs. 3(a) and 3(b) are weak due to the relatively small amounts of DBS in the samples, they show that the DBS molecules indeed organize into well-ordered submicron scale structures.

B. Dynamical mechanical analysis

In Fig. 4 is shown a typical result of a strain sweep experiment for a 0.5 wt % DBS/LC-E7 gel. Samples with a different DBS content show identical behavior (see Fig. 5). Before discussing the observations, two remarks are in place. First, the quantity $\gamma=\alpha_0 r/d$, plotted on the horizontal axes of Figs. 4–5, is the material strain experienced at the edges of the sample. This strain is larger by a factor of r/s than the strain experienced locally at a distance s from the center of the plates. Second, as mentioned in Sec. II, our analysis assumes linear viscoelastic behavior for which $\{G_d,\delta\}$ and $\{G',G''\}$ are strain-independent material constants.[21] This condition does not hold at large material strains, and consequently, the numerical values of G' and G'' have no significance outside the plateau regions of Figs. 4–5.

By comparing Figs. 4–5 to the literature data it is seen that the gel stiffness, embodied by G', agrees well with values reported for DBS/ethylene glycol[5] and DBS/siloxane gels.[6] Therefore, it is DBS and not the solvent which is responsible for the material stiffness, as was confirmed by a reference experiment on neat LC-E7. Since all samples examined show identical behavior as in Fig. 4, we conclude that for low ω, $G'\gg G''$ in DBS/LC-E7 gels. Thus, the gels are built from an almost perfectly elastic network that shows very little energy dissipation upon linear deformation.[21] However, upon increasing the deformation into the nonlinear strain regime (i.e., beyond the plateau region of Figs. 4–5), energy dissipation causes material failure, and original G' and G'' values could only be restored upon heating the material above T_{SG}.

The composition dependence of the mechanical properties of the gels is depicted in Fig. 5. The figure shows that the strain at failure γ_{max} decreases with increasing DBS content, while the gel stiffness G' and strength $\gamma_{max}\cdot G'$ increase. This may be understood by realizing that higher amounts of DBS are likely to form networks with finer mesh sizes and thicker fibers, which are less strainable, stiffer, and stronger.

Finally, observed gel strengths are in the range 600–2000 Pa (corresponding to loads of 6–20 g/cm^2). These values imply that gelled films can easily hold a top layer such as a glass plate or a polymer coating that may be *in situ* applied onto the film (e.g., in a continuous processing line). This, in our opinion, is indicative of the potential that thermoreversible LC gels have in large area applications.

C. Electro-optical characterization

In Fig. 6, a photograph of an 18 μm thick nonpixelated demonstrator cell with an area of 30×30 mm shows that the thermoreversible gel concept indeed allows us to create electro-optically active cells that are reversibly switchable at

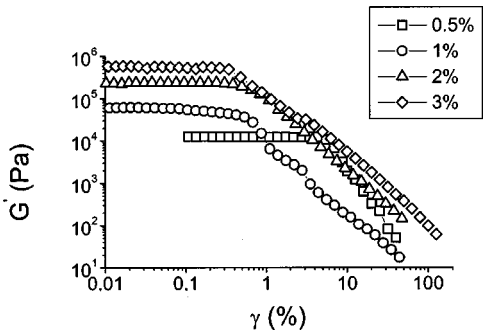

FIG. 5. Storage moduli vs material strain for gels of different DBS content at $T=30$ °C.

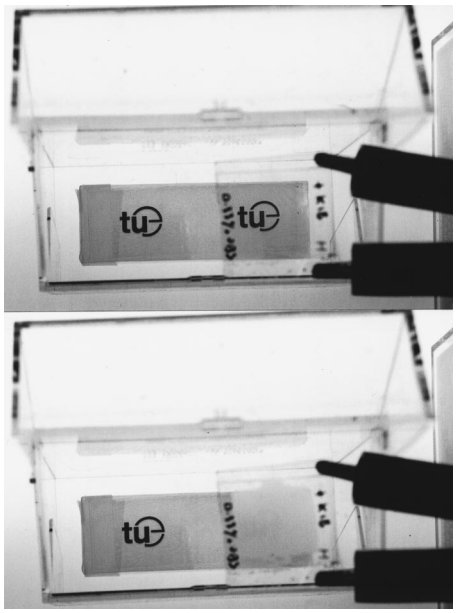

FIG. 6. The transparent on- (top) and light scattering off-state (bottom) of a 30×30 mm cell filled with a 1 wt % DBS/LC-E7 mixture. In the on state a 100 Hz ac voltage was supplied with the aid of a Keithley source measurement unit. In the photograph, the distance between the cell and the displayed symbol is approximately 10 cm.

100 V between a scattering-off and a transparent-on state. Clearly, both the clarity of the on-state and the amount of scattering in the off-state are promising with regard to application purposes. Benefits of the type of system explored by us, when compared to conventional PDLC systems, are its thermoreversibility (that may be explored in a continuous production line), the very low amounts of gelling agent needed, and the ease of gel manufacturing (in contrast to acrylate gels, no UV curing is needed). Additional benefits may lie in the large variety of gelling agents that have been discovered over the past years.[1] On the other hand, the operating voltage that is current required is high when compared to a PDLC reference cell, fully optimized at Philips Research.[26] This is shown in Fig. 7 which displays a selection of transmission versus applied voltage curves from a consecutive series of measurements. The figure also shows switching curves recorded after heating the cell to $T_{N/I}$ (dashed line) or T_{SG} (dotted line) and subsequent cooling. In the figure, the transmission is defined as $T=100I/I_0$, where I is the instantaneous transmission and I_0 the transmission of light passing an empty reference cell to correct for absorption losses due to the glass and ITO layers. Since the recorded transmissions are a strong function of illumination intensity and sample–source distance, we have monitored with the same setup the 7 μm reference PDLC cell (dash–dot line).[26] Although the difference in switching voltages between our cell and the PDLC cell is partially explained by a disparity in cell thickness ($V_{applied}$ scales linearly with d_{cell}) and partially by the fact that the PDLC film contains a fully optimized LC blend, it is clear that further optimization of our system is needed. In order to achieve this, control of phase separation (absence of residual amounts of DBS in the $\{N\}$ phase) and optimization of the properties of the $\{N+C_2\}$ interface are of utmost importance. Other aspects that need addressing are related to the contrast. We have observed that there is a loss of contrast (defined as the ratio of the highest and lowest transmission recorded) after first switching of the cell (Fig. 7), followed by a stabilization upon further use. Moreover, it was noticed that heating to $T_{N/I}$ and subsequent cooling leads to a reproducible, large contrast recovery, while ''melting'' the gel by heating to T_{SG} results in a complete recovery after cooling. Assuming that the loss of contrast upon first switching is caused by a ''permanent'' macroscopic reorganization of the network due to the forces imposed by the temporal homeotropical alignment of the LC molecules, it seems natural that heating to T_{SG}, at which ''gel melting'' occurs, completely restores the contrast. The reason why heating above $T_{N/I}$ has such a large effect is still somewhat obscure to us. The best explanation we can offer thus far is that after heating to $T_{N/I}$, the formation of a nematic liquid upon cooling exerts random distortions on the network, resulting in a partial loss of its macroscopic orientation.

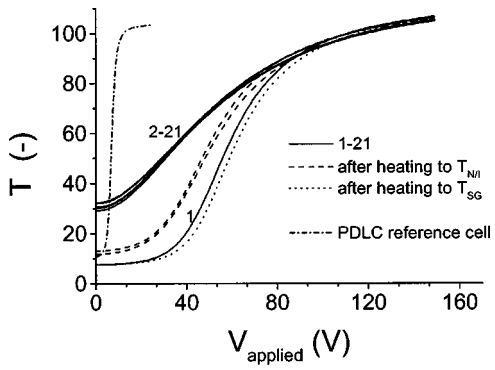

FIG. 7. Electro-optical characteristics of an 18 μm scattering cell containing a 1 wt % DBS/LC-E7 gel. Curves were obtained in a consecutive series of measurements in which the applied voltage was increased from 0 to 150 V every 0.1 s with 0.5 V. Dashed and dotted lines were recorded by the same procedure after heating the cells to, respectively, $T_{N/I}$ and T_{SG} and subsequent cooling. The dash–dotted line shows the characteristics of a fully optimized 7 μm PDLC cell as a reference.

Finally, it should be noted that in the demonstrator cell of Fig. 6 we only exploit the residual contrast residing after the first switching motion. It may be possible however to exploit the partial bistability observed in Fig. 7. Schemes for doing this have been proposed in the context of silica containing nematics.[19,27]

IV. CONCLUSIONS

The phase behavior of the thermoreversible LC gel forming system comprising the commercially available ingredients DBS and LC-E7 has been investigated by DSC and WAXS. It was found that the phase diagram displays a monotectic-type point, which we refer to as ''mesotectic,'' at which a liquid is in equilibrium with a solid and a mesophase. Further, it was shown that the location of the mesotectic point at extremely low weight fractions of DBS, combined with the demonstrated viscoelastic response of DBS/LC-E7, allows manufacturing of white light-scattering

films that are switchable to a clear state by ac electric fields. Finally, the electro-optical characteristics of a nonpixelated 30×30 demonstrator cell were presented.

ACKNOWLEDGMENTS

The authors gratefully acknowledge financial support from the Dutch Applied Science Foundation (Stichting Toegepaste Wetenschappen) and from ETH Zürich. They are also indebted to Dr. Jenci Kurja of Milliken Chemical for a generous supply of Millad 3905.

[1] P. Terech and R. G. Weiss, Chem. Rev. **97**, 3133 (1997).
[2] A. Thierry, C. Straupé, B. Lotz, and J. C. Wittmann, Polym. Commun. **31**, 299 (1990).
[3] S. Yamamoto, Kogyo Kagaku Zasshi **45**, 695 (1942).
[4] S. Yamasaki and H. Tsutsumi, Bull. Chem. Soc. Jpn. **68**, 123 (1995).
[5] M. Watase and H. Itagaki, Bull. Chem. Soc. Jpn. **71**, 1457 (1998).
[6] G. M. Smith and D. E. Katsoulis, J. Mater. Chem. **5**, 1899 (1995).
[7] H. Engelkamp, S. Middelbeek, and R. J. M. Nolte, Science **284**, 785 (1999).
[8] S. Yamasaki and H. Tsutsumi, Bull. Chem. Soc. Jpn. **68**, 146 (1995).
[9] R. Schlotmann and R. Walker, Kunststoffe **86**, 1002 (1996).
[10] T. A. Shepard, C. R. Delsorbo, R. M. Louth, J. L. Walborn, D. A. Norman, N. G. Harvey, and R. J. Spontak, J. Polym. Sci., Part B: Polym. Phys. **35**, 2617 (1997).
[11] W. Kurz and P. R. Sahm, *Gerichtet Erstarrte Eutektische Werkstoffe* (Springer, Berlin, 1975).
[12] R. H. C. Janssen, V. Stümpflen, C. W. M. Bastiaansen, D. J. Broer, T. A. Tervoort, and P. Smith, Jpn. J. Appl. Phys., Part 1 (in press).
[13] T. Kato, G. Kondo, and K. Hanabusa, Chem. Lett. **3**, 193 (1998).
[14] T. Kato, T. Kutsuna, K. Hanabusa, and M. Ukon, Adv. Mater. **10**, 606 (1998).
[15] N. Mizoshita, K. Hanabusa, and T. Kato, Adv. Mater. **11**, 392 (1999).
[16] H. G. Craighead, J. Cheng, and S. Hackwood, Appl. Phys. Lett. **40**, 22 (1982).
[17] J. W. Doane, N. A. Vaz, B.-G. Wu, and S. Žumer, Appl. Phys. Lett. **48**, 269 (1986).
[18] R. A. M. Hikmet, J. Appl. Phys. **68**, 4406 (1990).
[19] M. Kreuzer, T. Tschudi, W. H. de Jeu, and R. Eidenschink, Appl. Phys. Lett. **62**, 1712 (1993).
[20] H. V. Ivashchenko and V. G. Rumyantsev, Mol. Cryst. Liq. Cryst. **150A**, 1 (1987).
[21] J. D. Ferry, *Viscoelastic Properties of Polymers* (Wiley, Chichester, 1980).
[22] R. P. Feynman, *The Feynman Lectures on Physics* (Addison-Wesley, Reading, MA, 1964), Vol. 2, Chap. 38.
[23] M. D. Dadmun and M. Muthukumar, J. Chem. Phys. **98**, 4850 (1993).
[24] R. A. M. Hikmet and R. Howard, Phys. Rev. E **48**, 2752 (1993).
[25] R. H. C. Janssen, D. N. Theodorou, S. Raptis, and M. G. Papadopoulos, J. Chem. Phys. **111**, 9711 (1999).
[26] C. Serbutoviez, J. G. Kloosterboer, H. M. J. Boots, and F. J. Touwslager, Macromolecules **29**, 7690 (1996).
[27] R. Eidenschink and W. H. de Jeu, Electron. Lett. **27**, 1195 (1991).